# Learning Human-Object Interaction as Groups

**Jiajun Hong***, **Jianan Wei***, **Wenguan Wang**†
Zhejiang University
https://github.com/JiajunHong1/GroupHOI

## Abstract

Human-Object Interaction Detection (HOI-DET) aims to localize human-object pairs and identify their interactive relationships. To aggregate contextual cues, existing methods typically propagate information across all detected entities via self-attention mechanisms, or establish message passing between humans and objects with bipartite graphs. However, they primarily focus on pairwise relationships, overlooking that interactions in real-world scenarios often emerge from collective behaviors (*i.e.*, multiple humans and objects engaging in joint activities). In light of this, we revisit relation modeling from a *group* view and propose GroupHOI, a framework that propagates contextual information in terms of *geometric proximity* and *semantic similarity*. To exploit the geometric proximity, humans and objects are grouped into distinct clusters using a learnable proximity estimator based on spatial features derived from bounding boxes. In each group, a soft correspondence is computed via self-attention to aggregate and dispatch contextual cues. To incorporate the semantic similarity, we enhance the vanilla transformer-based interaction decoder with local contextual cues from HO-pair features. Extensive experiments on HICO-DET and V-COCO benchmarks demonstrate the superiority of GroupHOI over the state-of-the-art methods. It also exhibits leading performance on the more challenging Nonverbal Interaction Detection (NVI-DET) task, which involves varied forms of higher-order interactions within groups.

## 1 Introduction

> *No man is an island, entire of itself.*
>
> *– John Donne, Meditation XVII Devotions*

Human-Object Interaction Detection (HOI-DET), as a critical pillar in visual relationship understanding, identifies entities (*i.e.*, humans and objects) as basic building blocks, and leverages relationships as the connective glue that weaves them into meaningful patterns. Early works [1, 2] typically recognize `HO-pairs`, which are cropped from natural images by manually obtained bounding boxes, as composites (*i.e.*, visual phrases) in isolation. Recent efforts [3, 4] extend HOI reasoning to real-world scenarios involving `multiple entities` with complex relational structures. Building upon object detection frameworks, HOI-DET methods evolve alongside advancements in detector architectures from Faster R-CNN [5] to DETR-like variants [6, 7]. As a semantic interpretation task, HOI-DET can also benefit from large visual-linguistic models (*e.g.*, CLIP [8] and BLIP [9]) pre-trained on extensive image-text corpora. Despite architectural innovations and multi-modal knowledge transfer, the core challenge remains unchanged: ❶*how to structure and reason about relationships among entities?*

Current methods [3, 10, 11] primarily reason over global context via the self-attention mechanism (Fig. 1(a)), while another strand of research constrains information exchange within homogeneous entities (*i.e.*, human-human, object-object) [12, 13] or heterogeneous neighborhoods (*i.e.*, human-object, object-human) [11] via bipartite graph (Fig. 1(b)). Despite achieving impressive performance,

* The first two authors contribute equally to this work.
† Corresponding Author: Wenguan Wang.

39th Conference on Neural Information Processing Systems (NeurIPS 2025).

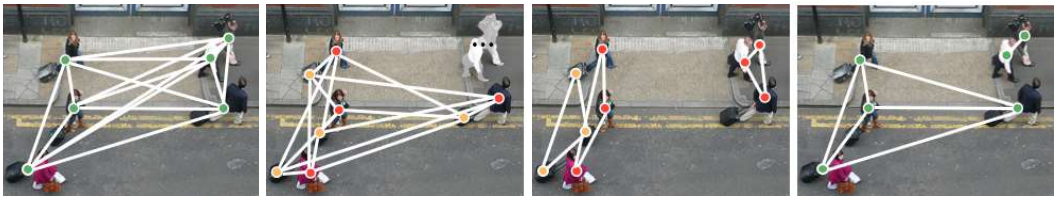

(a) Complete Graph (b) Bipartite Graph (c) Geometric Graph (d) Semantic Graph

Figure 1: **Relation modeling paradigms**. While existing methods primarily model relations using complete (a) or bipartite (b) graphs, our approach introduces geometric (c) and semantic (d) graphs, enabling more structured and context-aware relational reasoning. ●, ●, and ● denote humans, objects, and interactions, respectively.

these methods remain confined to the modeling of predefined pairwise relations, leaving the inherent collective patterns [14] (*i.e.*, multiple entities engaging in joint activities) between entities unexplored.

Tackling this notable void brings us back to the classical clustering view for structuring and organizing visual entities by finding groups of similar ones, *i.e.*, **detecting HOIs as groups**. Tomasello's theory of shared intentionality [15] posits that with joint goals ("we-mode") and role coordination, participants tend to draw close to each other and perform collaborative actions. Considering a busy street with numerous pedestrians (Fig. 1), even without their explicit interpersonal relationships or social affiliations, the individuals can be naturally categorized into distinct groups based on their spatial proximity (Fig. 1(c)). Moreover, the walkers *pulling suitcases* typically exhibit similar visual characteristics—walking forward with swinging arms and suitcases trailing behind them—highlighting their shared behavior (Fig. 1(d)). Hence question ❶ becomes more fundamental from a group view: ❷ *how is a group formed?* and ❸ *how does a group function?*

Driven by question ❷, we construct social groups guided by the Gestalt grouping principles of Proximity and Similarity [16]: **First**, the ***geometric proximity principle***, *i.e.*, the tendency for individuals to form groups with those physically close to, is implemented by constructing *geometric groups* based on the central distance and Intersection over Union (IoU) of bounding boxes. **Second**, the ***semantic similarity principle***, *i.e.*, the tendency for individuals to affiliate with those sharing visual characteristics or behavioral patterns, is operationalized through building *semantic groups* of interaction proposals based on similarity of their feature embeddings. Notably, groups in social environments demonstrate complex and diverse compositions with overlapping memberships, which complicates quantification and modeling. To address this, we treat each proposal and its neighbors as a distinct group, establishing a one-to-one correspondence between groups and proposals.

To address question ❸, we propose GroupHOI, a HOI detector that enhances interaction reasoning by discovering inherent group patterns within visual scenes. Building on DETR [17], we model two distinct group structures to capture contextual dependencies: **First**, based on object detection outputs, we construct geometric groups for each entity and perform structure-aware reasoning via soft correspondence through self-attention, enabling fine-grained aggregation and targeted dissemination of local cues (§3.3). **Second**, we construct semantic groups to extract localized interaction priors, which are then integrated into the interaction decoder via a pooling operator to enable context-aware reasoning through a structured local-global processing scheme (§3.4). Visualizations in §4.5 provide transparency into how contextual dependencies are organized and leveraged.

To conclude, our contributions are: **i)** defining two visual attraction principles to construct groups; **ii)** proposing a one-stage framework that integrates these principles into HOI-DET; **iii)** endowing the HOI detector with enhanced interpretability via grouping mechanisms.

Our method is evaluated on two standard HOI-DET benchmarks: V-COCO [18] and HICO-DET [2], achieving impressive performance with **36.70** mAP on HICO-DET and **65.0** mAP on V-COCO. It surpasses the state-of-the-art method (*i.e.*, Pose-Aware [19]) by solid margins, *i.e.*, **+0.84** and **+3.9** mAP. Moreover, it achieves leading performance on the more challenging Nonverbal Interaction Detection (NVI-DET) [20] task, which permits diverse forms of higher-order group interactions. On the NVI benchmark [20], it reaches **73.19** AR on `val` and **75.21** AR on `test`.

## 2 Related Work

**Human-Object Interaction Detection.** Current HOI detectors can be categorized into two-stage and one-stage paradigms. Two-stage methods [1, 2, 21–28] typically employ off-the-shelf detectors (*e.g.*,

Faster R-CNN [5]) to locate humans and objects, then generate human-object pairs for interaction recognition. In contrast, one-stage methods [29–39], inspired by DETR [6], reformulate the task as a set prediction problem, and perform end-to-end triplets detection without explicit pairing. Recent studies [3, 4, 40–44] show strong gains by transferring knowledge from models pre-trained on large-scale image-text corpora (*e.g.*, CLIP [8], BLIP [9], and Stable Diffusion [45]) or large language models (*e.g.*, OPT [46]). Instead of focusing solely on architectural innovations or large-scale knowledge transfer, our approach highlights a complementary perspective on relation modeling, emphasizing how to organize and structure relations among entities.

**Relation Modeling for Detection Tasks.** Early object detectors [47–49] mainly built upon R-CNN family to localize and recognize each object in isolation, without contextual information exchange. To tackle this issue, [50] proposes a cascaded multi-stage framework with group recursive learning, while [51] incorporates global context across local regions. Recently, transformer-based methods such as DETR [6] reformulate detection as a set prediction problem, using self-attention to aggregate global context and enhance relational reasoning. HOI-DET methods have undergone a similar evolution. Early two-stage HOI-DET methods [23–25] confine information sharing to pre-defined human-object pairs and restrict interaction reasoning to isolated triplets, while DETR-based HOI-DET methods [30–32] leverage self-attention mechanisms to enable more comprehensive relational reasoning. Graph-based approaches [11, 13, 52–56] construct fully connected or bipartite graphs to facilitate message passing between entities. Building on this idea, several recent works [57, 58] further explore hypergraph representations, offering a more expressive way for high-order relations. However, most of them prioritize *how to reason about relations across entities* while neglecting *how to structure the relations among them*, thereby introducing noise from spurious correlations.

**Group Analysis for Vision Tasks.** Groups, as the fundamental units of human society, have become a pivotal analysis tool to understand complex human-centric scenes, with applications in crowd analysis, pedestrian trajectory prediction, and collective activity recognition. In crowd analysis, group-based methods [59] treat groups as atomic units of the scene, while individual-group methods [60] seek to leverage collective human information rather than processing them in isolation. Recently, PANDA [61] dataset enriched the task by integrating global context, high-resolution localized details, and temporal activity patterns, providing rich and hierarchical annotations. For pedestrian trajectory prediction, a number of existing approaches [57, 62–64] aim to improve multi-person tracking by incorporating group relationships. For instance, GroupNet [57] addresses the multi-agent trajectory prediction problem by leveraging multiscale hypergraphs to model both pairwise and group-level interactions more effectively. Collective activity recognition principally aims to capture the nuances of multi-human interactions in wide field-of-view scene, prompting many explorations of intra-group dynamics. For instance, ARG [65] tries to model both appearance and spatial dependencies between humans, and SAM [66] builds a dense relation graph and prunes it to a sparse one.

Inspired by these endeavors, we revisit HOI-DET from a group perspective, explore the visual principles underlying group formation, and propose a dedicated framework designed to operationalize these principles for HOI-DET, while introducing little extra computational overhead.

# 3 Methodology

## 3.1 Preliminary

Prevailing HOI-DET methods [3, 4, 19, 67, 68] employ a standardized DETR-based [69] pipeline for instance detection. Given an input image $\boldsymbol{I}$ with position embeddings $\boldsymbol{P}_e$, a visual encoder preceded by a CNN backbone is applied to extract features $\boldsymbol{V}_e$. Then, an instance decoder $\mathcal{D}_{ins}$ is employed to transform human $\boldsymbol{Q}_h$ and object $\boldsymbol{Q}_o$ queries into the outputs by retrieving the encoded features $\boldsymbol{V}_e$:

$$[\boldsymbol{Q}'_h, \boldsymbol{Q}'_o] = \mathcal{D}_{ins}(\boldsymbol{V}_e, \boldsymbol{Q}_h, \boldsymbol{Q}_o), \tag{1}$$

where $\boldsymbol{Q}'_h, \boldsymbol{Q}'_o$ are then processed into bounding boxes $\boldsymbol{B}_h, \boldsymbol{B}_o$ and object class labels $\boldsymbol{L}_o$. In the interaction branch, human $\boldsymbol{Q}'_h$ and object $\boldsymbol{Q}'_o$ outputs are exhaustively enumerated [33, 68] or directly associated [3, 67, 69] to form HO-pairs and interaction queries $\boldsymbol{Q}_{ins}$ for interaction classification.

## 3.2 Rethinking the Relation Modeling in HOI-DET

**Revisiting Transformer-based Relation Modeling.** Building upon DETR [69], most transformer-based HOI-DET models [3, 10, 11] perform global relational modeling among all the entity candidates

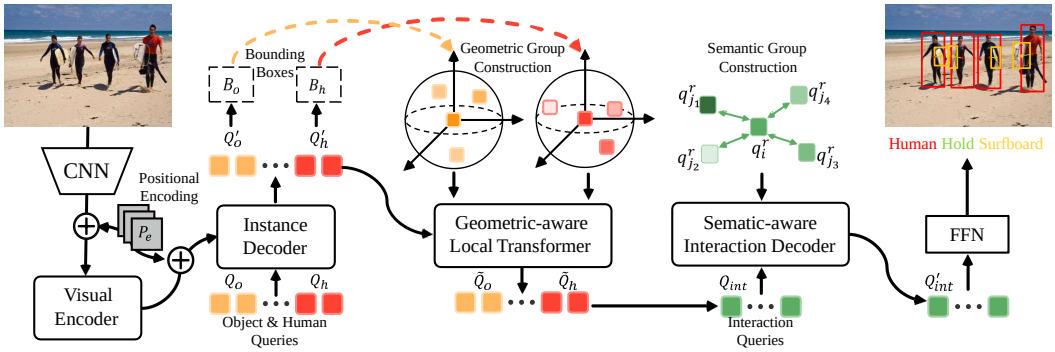


Figure 2: **Overview of GroupHOI**. GroupHOI comprises three key modules: **i)** a visual encoder extracts features, followed by an instance decoder to locate human-object pairs; **ii)** a geometric-aware local transformer aggregates and distributes contextual information within geometric groups; **iii)** a semantic-aware interaction decoder leverages local-global semantic dependencies for interaction prediction.

or their compositions via attention, which inherently establish a ***fully-connected graph*** for information exchange. Specifically, given an entity candidate $\boldsymbol{q}_i^e \in \boldsymbol{Q}_e = \boldsymbol{Q}'_h \cup \boldsymbol{Q}'_o$, the relational modeling is achieved by the transformer decoder through self-attention operations with all entity queries:

$$\hat{\boldsymbol{q}}_i^e = \sum\nolimits_{\boldsymbol{q}_j^e \in \boldsymbol{Q}_e} \texttt{Softmax}(\boldsymbol{q}_i^e \cdot \boldsymbol{q}_j^e) \cdot \boldsymbol{q}_j^e, \tag{2}$$

where `Softmax` propagates contextual cues by establishing soft correspondences from a global view, $\boldsymbol{q}_j^e \in \boldsymbol{Q}_e$ denotes all the detected entities.

**Revisiting Graph-based Relation Modeling.** Another line of research [11–13, 32, 54] constructs graphs based on the detected entities to enable relational modeling. Each node $\boldsymbol{q}_i^e$ is connected to a predefined set of neighboring nodes $\mathcal{N}_i$ and exchanges contextual information via message passing:

$$\hat{\boldsymbol{q}}_i^e = \boldsymbol{q}_i^e + \sigma(\sum\nolimits_{\boldsymbol{q}_j^e \in \mathcal{N}_i} \alpha_{ij} \cdot \texttt{MessagePassing}(\boldsymbol{q}_i^e, \boldsymbol{q}_j^e)), \tag{3}$$

where $\sigma$ is the activation function, $\alpha$ is an adjacency weight between nodes, and `MessagePassing` denotes the message passing function. In terms of the set of neighboring nodes $\mathcal{N}(i)$, many studies [12, 13] define it as the union of all other entities in the scene, resulting in a ***fully-connected graph*** comprising both human and object nodes, while others [11, 13, 32, 54] restrict it to heterogeneous entities (*i.e.*, human-object, object-human), thereby formulating a ***bipartite graph***.

Though effective, these methods either treat all the entities as a single group or crudely partition them into two homogeneous groups. However, real-world scenarios demonstrate greater complexity in collective patterns: picture a cocktail party where a cluster of guests holding wine glasses or bottles is debating heatedly, while individuals seated on chairs around the venue are eating pizza. Given this divergence, we propose learning HOI as groups guided by the Gestalt grouping principles [16]: the *geometric proximity principle* and *semantic similarity principle*. The former is operationalized by *learning entities as geometric groups*, and the latter by *learning interactions as semantic groups*.

### 3.3 Learning Entities as Geometric Groups

According to Gestalt psychology [16], the proximity principle states that spatially adjacent elements are naturally perceived as coherent groups. This perceptual tendency has been applied as a strong inductive bias for structuring visual scenes [70]. Motivated by this principle, we extend it to HOI-DET by constructing geometric groups that organize detected entities based on their spatial configurations.

**Geometric Group Construction.** We construct groups for each entity embedding $\boldsymbol{q}_i^e$ by selecting its $K^g$ nearest neighbor entities based on the geometric distance of their corresponding bounding boxes $\boldsymbol{B}$ obtained by the instance decoder. However, simple geometric metrics often fall short in capturing the diverse sizes and spatial configurations of bounding boxes. To address this, we introduce a learnable estimator to measure geometric proximity among bounding boxes. First, we formulate the spatial feature $\boldsymbol{f}_{i,j}^p = [dis_{i,j}, IoU_{i,j}]$ by concatenating two geometric properties: **i)** the Euclidean distance $dis_{i,j}$ between the centroids of two bounding boxes $\boldsymbol{c}_i$ and $\boldsymbol{c}_j$ (*i.e.*, $dis_{i,j} = \sqrt{(\Delta \boldsymbol{c}_{i,j}^x)^2 + (\Delta \boldsymbol{c}_{i,j}^y)^2}$, where $\Delta \boldsymbol{c}_{i,j}^x = \boldsymbol{c}_i^x - \boldsymbol{c}_j^x$ and $\Delta \boldsymbol{c}_{i,j}^y = \boldsymbol{c}_i^y - \boldsymbol{c}_j^y$), and **ii)** the IoU between two

bounding boxes $\boldsymbol{B}_i$ and $\boldsymbol{B}_j$, *i.e.*, $IoU_{i,j} = |\boldsymbol{B}_i \cap \boldsymbol{B}_j|/|\boldsymbol{B}_i \cup \boldsymbol{B}_j|$. Then, a simple linear layer is employed to compute the proximity score $s_{i,j}$ from $\boldsymbol{f}^p_{i,j}$ and yields a proximity score matrix. In this matrix, lower scores indicate closer spatial proximity. For each entity, we select the $K^g$ neighbors with the lowest scores to construct its geometric neighbor set $N^g_i$.

**Geometric Context Aggregation and Dispatch.** GroupHOI adopts a *geometric-aware local transformer* to capture the contextual cues from unordered entities by applying self-attention locally. First, to preserve the relative positional information within groups, we introduce trainable, parameterized position encodings $\boldsymbol{p}_{i,j}$ as follows:

$$\boldsymbol{p}_{i,j} = \delta(\boldsymbol{q}^e_i - \boldsymbol{q}^e_j), \tag{4}$$

where $\delta$ is a two-layer MLP with ReLU nonlinearity. Then, we compute the dispatch matrix $\boldsymbol{t}_{i,j}$ for each entity:

$$\boldsymbol{t}_{i,j} = \texttt{Softmax}(\gamma(\phi_1(\boldsymbol{q}^e_i) - \phi_2(\boldsymbol{q}^e_j) + \boldsymbol{p}_{i,j})), \tag{5}$$

where $\phi_1$ and $\phi_2$ are linear projections to perform point-wise feature transformation, and $\gamma$ is an MLP to produce the subtraction relation. Based on dispath matrix, GroupHOI adaptively aggregates the contextual cues within groups and utilizes them to update the entity embeddings:

$$\tilde{\boldsymbol{q}}^e_i = \theta(\textstyle\sum_{\boldsymbol{q}^e_j \in \mathcal{N}^g_i} \boldsymbol{g}_{i,j} \odot (\phi_3(\boldsymbol{q}^e_j) + \boldsymbol{p}_{i,j})) + \boldsymbol{q}^e_i, \tag{6}$$

where $\phi_3$ is a linear projection, and $\theta$ denotes a feature alignment function. This process is applied among homogeneous entities, yielding $\tilde{\boldsymbol{Q}}_h$ and $\tilde{\boldsymbol{Q}}_o$ for human and object embeddings, respectively.

### 3.4 Learning Interactions as Semantic Groups

The concept of semantic grouping has long been recognized in cognitive science as a fundamental mechanism by which humans perceive and organize the world. According to Gestalt principles [16], humans naturally group elements based on contextual similarity to reduce cognitive load and enable efficient reasoning. Inspired by this insight, we incorporate semantic-aware grouping into interaction reasoning and enhance the vanilla transformer decoder with semantic-aware local cues.

**Semantic Group Construction.** We first initialize the interaction queries $\boldsymbol{Q}_{int}$ by computing the mean of $\tilde{\boldsymbol{Q}}_h$ and $\tilde{\boldsymbol{Q}}_o$. Given the complex and diverse group structures with overlapping memberships in social environments, we avoid using traditional partitioning techniques like $k$-means clustering to construct groups. Instead, we formulate distinct groups $\mathcal{N}^s_i$ for each interaction query $\boldsymbol{q}^r_i \in \boldsymbol{Q}_{int}$ by assessing pairwise cosine similarity $\boldsymbol{sim}_{ij} = (\boldsymbol{q}^r_i \cdot \boldsymbol{q}^r_j)/(||\boldsymbol{q}^r_i||||\boldsymbol{q}^r_j||)$ between it and other queries $\boldsymbol{q}^r_j$ and selecting its top-$K^s$ most similar counterparts.

**Semantic Context Aggregation.** Given each query $\boldsymbol{q}^r_i$ with its semantic group $\mathcal{N}^s_i$, we utilize max pooling to aggregate semantic message from its group members $\boldsymbol{q}^r_j$:

$$\boldsymbol{m}_i = \texttt{max}(\phi_4(\boldsymbol{q}^r_i, \boldsymbol{q}^r_j - \boldsymbol{q}^r_i)), \quad \boldsymbol{q}^r_j \in \mathcal{N}^s_i, \tag{7}$$

where $\phi_4$ represents a sequence of linear layers, batch normalization, and ReLU layers.

**Local-Global Integration.** As described in §3.2, the transformer-based interaction decoder models global relations through self-attention but lacks explicit local relation modeling. To address this limitation, we construct a *semantic-aware interaction decoder* by integrating the proposed local semantic context aggregation mechanism into the naive decoder, which enhances its capacity for interaction reasoning. Specifically, prior to each decoder layer, the local semantic context is aggregated and incorporated into the original query via residual connection:

$$\hat{\boldsymbol{q}}^r_i = \boldsymbol{q}^r_i + \phi_5(\boldsymbol{m}_i), \tag{8}$$

where $\phi_5$ shares the same identity structure as $\phi_4$. $\hat{\boldsymbol{q}}^r_i$ is subsequently passed through the self-attention and cross-attention modules in the interaction decoder layer.

### 3.5 Implementation Details

**Network Architecture.** To ensure fair comparison with previous HOI-DET methods [3, 4, 67, 71], we adopt ResNet-50 [72] as the visual backbone. Our transformer-based architecture consists of a 6-layer encoder, a 3-layer instance decoder, and a 3-layer interaction decoder. Following [3, 4], we initialize 64 learnable queries for human and object branches, and set the feature dimensions to

256 for human/object representations and 768 for interaction representations. We perform group construction independently at each layer of both the instance and interaction decoders, where the geometric and semantic group sizes are set to 4 and 2. We evaluate three variants of GroupHOI using different pre-trained VLMs: **i)** CLIP (ViT-B/16) [8], **ii)** CLIP (ViT-L/14), and **iii)** BLIP2 (ViT-L) [9]. In each variant, we follow [3, 4] to initialize the classification heads using VLM text embeddings and integrate visual features from the VLM visual encoder into the interaction decoder.

**Training Objectives.** Following [3, 4], our model is optimized by the following loss:

$$\mathcal{L}_{\text{HOI}} = \lambda_b \mathcal{L}_b + \lambda_u \mathcal{L}_u + \lambda_c^o \mathcal{L}_c^o + \lambda_c^a \mathcal{L}_c^a, \tag{9}$$

where $\mathcal{L}_b$ denotes the box regression loss, $\mathcal{L}_u$ indicates the intersection-over-union loss, $\mathcal{L}_c^o$ and $\mathcal{L}_c^a$ represent the cross-entropy loss for object and interactions classification, respectively. The coefficient factors $\{\lambda_b, \lambda_u, \lambda_c^o, \lambda_c^a\}$ are empirically set as $\{2.5, 1, 1, 1\}$.

**Reproducibility.** GroupHOI is implemented in PyTorch. The model is trained with a batchsize of 8 for 90 epochs on 2 GeForce RTX 4090 GPUs.

# 4 Experiment

## 4.1 Experiments on HOI-DET

**Datasets.** We conduct experiments on V-COCO [18] and HICO-DET [2]:

- **V-COCO** is a specialized subset of MS-COCO [73], which comprises 10,346 images (5,400 for training and 4,946 for testing). The dataset annotates 263 unique human-object interactions, covering 29 action categories and 80 object categories.
- **HICO-DET** comprises a total of 47,776 images, with 38,118 designated for training and 9,658 for testing. It includes 80 object categories, consistent with those in V-COCO dataset, 117 action categories and 600 distinct HOI classes.

**Evaluation Metrics.** We employ mAP as our evaluation metric. For V-COCO [18], mAP is reported under two different scenarios: scenario 1 for all 29 action categories, and scenario 2 which excludes 4 body motion categories. For HICO-DET [2], we evaluate GroupHOI in complete 600 HOI categories (Full), the 138 rare categories with fewer than 10 training instances (Rare), and remaining 462 categories (Non-Rare). For each object, mAP is computed in the whole dataset (Default) and subset containing the object (Known Object).

**Training.** Our backbone is initialized with DETR [6] pre-trained on MS-COCO [73]. The model is trained using AdamW optimizer [74] with a batchsize of 8 for 90 epochs. The initial learning is set to $5e^{-5}$, which reduces by a factor of 10 every 30 epochs.

**Testing.** For fairness, GroupHOI operates without data augmentation. We retain the top-$K$ HOI candidates ($K = 100$) followed by Non-Maximum Suppression for redundancy removal.

**Quantitative Results on HICO-DET.** As shown in Table 1, our model with a VIT-B/16 CLIP [8] variant already outperforms all the competitors under the same setting by a substantial margin. In particular, GroupHOI surpasses the previous state-of-the-art Pose-Aware [19] by **0.84/2.38/0.40** mAP on the Full, Rare, and Non-Rare settings. Notably, GroupHOI exhibits a comparable number of parameters and FLOPs to HOICLIP [4] (§4.3), but delivers substantial improvements of **2.11/3.74/1.52** mAP on HICO-DET [2]. Moreover, leveraging more powerful VLMs, *i.e.*, ViT-L/14 CLIP [8] and ViT-L BLIP2 [9], GroupHOI boosts its performance and sustains state-of-the-art results. Both with ViT-L/14 CLIP, GroupHOI suppresses CMMP [68] by a large margin with **1.32** mAP under Full, while it narrowly trails CMMP in Rare setting. Compared to UniHOI [40] which retrieves knowledge from large language models, GroupHOI with ViT/L BLIP2 still leads by **0.47/ 0.71/0.39** mAP.

**Quantitative Results on V-COCO.** For V-COCO, GroupHOI exhibits competitive performance but remains slightly inferior to STIP [33], VIL [75], and CQL [76]. However, on HOI-DET, our method surpasses them by a solid margin. We attribute this to GroupHOI's improved capability in handling more complex interactions, as evidenced by: HOI-DET contains 600 HOI interactions (*vs*.293 in V-COCO), an average of 4 interactions (*vs*.3 in V-COCO) and 6 entities per sample (*vs*.4 in V-COCO).

Table 1: **Quantitative results** on HICO-DET [2] `test` and V-COCO [18] `test`. DF and KO denote the Default and Known Object evaluation settings of HICO-DET. CLIP/B16, CLIP/B32, CLIP/L14 represent VIT-B/16, VIT-B/32 and VIT-L/14 settings for CLIP respectively. See §4.1 for details.

| Method | Config | HICO-DET (DF) | | | HICO-DET (KO) | | | V-COCO | |
|---|---|---|---|---|---|---|---|---|---|
| | | Full | Rare | Non-Rare | Full | Rare | Non-Rare | $AP^{S1}_{role}$ | $AP^{S2}_{role}$ |
| QPIC [67] [CVPR21] | R50 | 29.07 | 21.85 | 31.23 | 31.68 | 24.14 | 33.93 | 58.8 | 61.0 |
| QPIC [67] [CVPR21] | R101 | 29.90 | 23.92 | 31.69 | 32.38 | 26.06 | 34.27 | 58.3 | 60.7 |
| HOTR [69] [CVPR21] | R50 | 23.46 | 16.21 | 25.60 | - | - | - | 55.2 | 64.4 |
| CDN(S) [17] [NeurIPS21] | R50 | 31.44 | 27.39 | 32.64 | 34.09 | 29.63 | 35.42 | 61.2 | 63.8 |
| CDN(B) [17] [NeurIPS21] | R50 | 31.78 | 27.55 | 33.05 | 34.53 | 29.73 | 35.96 | 62.3 | 64.4 |
| CDN(L) [17] [NeurIPS21] | R101 | 32.07 | 27.19 | 33.53 | 34.79 | 29.48 | 36.38 | 63.9 | 65.9 |
| MSTR [77] [CVPR22] | R50 | 31.17 | 25.31 | 32.92 | 34.02 | 28.83 | 35.57 | 62.0 | 65.2 |
| STIP [33] [CVPR22] | R50 | 32.22 | 28.15 | 33.43 | 35.29 | 31.43 | 36.45 | **65.1** | **69.7** |
| PViC [71] [ICCV23] | R50 | 34.69 | 32.14 | 35.45 | 38.14 | 35.38 | 38.97 | 62.8 | 67.8 |
| Pose-Aware [19] [CVPR24] | R50 | **35.86** | **32.48** | **36.86** | **39.48** | **36.10** | **40.49** | 61.1 | 66.6 |
| DOQ [78] [CVPR22] | R50+CLIP/B16 | 33.28 | 29.19 | 34.50 | - | - | - | 63.5 | - |
| GEN-VLKT [3] [CVPR22] | R50+CLIP/B16 | 33.75 | 29.25 | 35.10 | 37.80 | 34.76 | 38.71 | 62.4 | 64.4 |
| ADA-CM [79] [ICCV23] | R50+CLIP/B16 | 33.80 | 31.72 | 34.42 | - | - | - | 56.1 | 61.5 |
| HOICLIP [4] [CVPR23] | R50+CLIP/B32 | 34.59 | 31.12 | 35.74 | 37.61 | 34.47 | 38.54 | 63.5 | 64.8 |
| VIL [75] [ACMMM23] | R50+CLIP/B16 | 34.21 | 30.58 | 35.30 | 37.67 | 34.88 | 38.50 | 65.3 | 67.7 |
| CQL [76] [CVPR23] | R50+CLIP/B16 | 35.36 | 32.97 | 36.07 | - | - | - | **66.4** | **69.2** |
| LOGICHOI [38] [NeurIPS23] | R50+CLIP/B16 | 35.47 | 32.03 | 36.22 | 38.21 | 35.29 | 39.03 | 64.4 | 65.6 |
| CMMP [68] [ECCV24] | R50+CLIP/B16 | 33.24 | 32.26 | 33.53 | - | - | - | - | 61.2 |
| HOIGen [68] [ACMMM24] | R50+CLIP/B16 | 34.84 | 34.52 | 34.94 | - | - | - | - | - |
| CEFA [80] [ACMMM24] | R50+CLIP/B16 | 35.00 | 32.30 | 35.81 | 38.23 | 35.62 | 39.02 | 63.5 | - |
| GroupHOI (ours) | R50+CLIP/B16 | **36.70** | **34.86** | **37.26** | **39.42** | **37.78** | **39.91** | 65.0 | 66.0 |
| ADA-CM [79] [ICCV23] | R50+CLIP/L14 | 38.40 | 37.52 | 38.66 | - | - | - | 58.6 | 64.0 |
| UniVRD [81] [ICCV23] | R50+CLIP/L14 | 37.41 | 28.90 | 39.95 | - | - | - | - | - |
| CMMP [68] [ECCV24] | R50+CLIP/L14 | 38.14 | **37.75** | 38.25 | - | - | - | - | 64.0 |
| GroupHOI (ours) | R50+CLIP/L14 | **39.46** | 37.10 | **40.16** | **41.58** | **39.42** | **42.40** | **66.4** | **67.3** |
| UniHOI [40] [NeurIPS23] | R50+BLIP2 | 40.06 | 39.91 | 40.11 | 42.20 | 42.60 | 42.08 | 65.6 | **68.3** |
| GroupHOI (ours) | R50+BLIP2 | **40.53** | **40.62** | **40.50** | **42.70** | **42.92** | **42.64** | **66.4** | 67.8 |

### 4.2 Experiments on NVI-DET

**Task Formulation.** Given an input image, it predicts a set of ⟨*individual*, *group*, *interaction*⟩ triplets, aiming to localize each individual and identify the social group it belongs to, while determining the category of its nonverbal interaction. Unlike HOI-DET [18] that focuses on recognizing actions between human-object pairs, NVI-DET models interactions in a more flexible and generalized manner. Specifically, it accounts for interactions involving arbitrary numbers of humans, which makes the task significantly more challenging.

**Dataset.** NVI [20] densely labeling social groups in pictures, along with 22 atomic-level nonverbal behaviors (16 individual- and 6 group-wise) under five broad interaction types. It contains 13,711 images in total and splits them into 9,634, 1,418 and 2,659 for train, val and test.

**Evaluation Metrics.** Consistent with [20], we utilize mean Recall@K (mR@K) for evaluation. Specifically, we report mR@25, mR@50, and mR@100 under different IoU thresholds for matching predictions with ground truth, along with their average (AR) to provide a comprehensive evaluation.

**Quantitative Results.** Following [20], we compare GroupHOI with modified versions of three state-of-the-art HOI-DET methods (*i.e.*, $m$-QPIC [67], $m$-CDN [17], and $m$-GEN-VLKT [3]) and NVI-DEHR [20] on NVI [20]. As shown in Table 2, GroupHOI surpasses all other methods, reaching **73.19** and **75.21** AR on NVI `val` and `test`. Furthermore, we analyze performance across individual-wise and group-wise interactions. Table 3 shows our model consistently outperforms others by significant margins in both sets. These results verify our model's effectiveness in identifying social group structures and capturing the collective behaviors within them.

### 4.3 Diagnostic Experiments

As shown in Table 4, we conduct a set of ablation studies on HICO-DET [2] for deeper analysis.

Table 2: **NVI-DET results** on NVI [20] `val` and `test`. See §4.2 for details.

| Method | val | | | | test | | | |
|---|---|---|---|---|---|---|---|---|
| | mR@25 | mR@50 | mR@100 | AR | mR@25 | mR@50 | mR@100 | AR |
| $m$-QPIC [67] [CVPR21] | **56.89** | 69.52 | 78.36 | 68.26 | 59.44 | 71.46 | 80.07 | 70.32 |
| $m$-CDN [17] [NeurIPS21] | 55.57 | 71.06 | 78.81 | 68.48 | 59.01 | 72.94 | 82.61 | 71.52 |
| $m$-GEN-VLKT [3] [CVPR22] | 50.59 | 70.87 | 80.08 | 67.18 | 56.68 | 74.32 | 84.18 | 71.72 |
| NVI-DEHR [20] [ECCV24] | 54.85 | 73.42 | 85.33 | 71.20 | 59.46 | 76.01 | **88.52** | 74.67 |
| GroupHOI (ours) | 55.67 | **76.73** | **87.16** | **73.19** | **62.67** | **76.57** | 86.42 | **75.21** |

Table 3: **Individual-** and **group-wise** interactions results on NVI [20] `val`. See §4.2 for details.

| Method | individual | | | | group | | | |
|---|---|---|---|---|---|---|---|---|
| | mR@25 | mR@50 | mR@100 | AR | mR@25 | mR@50 | mR@100 | AR |
| $m$-QPIC [67] [CVPR21] | **52.23** | 66.09 | 75.98 | 64.77 | 69.18 | 78.62 | 84.85 | 77.55 |
| $m$-CDN [17] [NeurIPS21] | 50.67 | 68.23 | 76.74 | 65.21 | 68.66 | 78.60 | 84.34 | 77.20 |
| $m$-GEN-VLKT [3] [CVPR22] | 44.98 | 68.51 | 78.30 | 63.93 | 67.84 | 79.47 | 87.12 | 78.14 |
| NVI-DEHR [20] [ECCV24] | 49.37 | 70.04 | 83.82 | 67.74 | 69.47 | 82.45 | 89.35 | 80.42 |
| GroupHOI (ours) | 49.60 | **74.03** | **85.63** | **69.75** | **71.87** | **83.92** | **91.24** | **82.34** |

**Analysis of Key Modules.** We analyze the effects of geometric and semantic groups in our framework. As shown in Table 4 (a), the results indicate that: **First**, both geometric and semantic relation learning contribute to HOI prediction. Incorporating geometric and semantic groups individually yields mAP gains of **0.67/0.91/0.81** and **0.21/0.45/0.31** under Full/Rare/Non-Rare settings respectively. **Second**, the combination of them yields optimal performance, delivering **0.98/2.66/0.70** mAP improvements over the baseline, which highlights a more comprehensive relation modeling in HOI prediction.

Table 4: **Ablation study** of GroupHOI on HICO-DET [2] `test`, where GEO and SEM represent geometric group and semantic group, *Homo.* and *Hetero.* mean homogeneous group and heterogeneous group (§4.3).

(a) Analysis of key modules

| GEO | SEM | Full | Rare | Non-Rare |
|---|---|---|---|---|
| - | - | 35.72 | 32.20 | 36.56 |
| ✓ | - | 36.39 | 33.11 | 37.37 |
| - | ✓ | 35.93 | 32.65 | 36.87 |
| ✓ | ✓ | **36.70** | **34.86** | **37.26** |

(b) Analysis of geometric group size

| Group Size | Full | Rare | Non-Rare |
|---|---|---|---|
| $K^g = 2$ | 36.23 | 32.97 | 37.13 |
| $K^g = 3$ | 36.34 | 33.87 | 37.32 |
| $K^g = 4$ | **36.70** | **34.86** | **37.26** |
| $K^g = 5$ | 36.45 | 33.57 | 36.95 |

(c) Analysis of semantic group size

| Group Size | Full | Rare | Non-Rare |
|---|---|---|---|
| $K^s = 1$ | 36.07 | 32.09 | 37.26 |
| $K^s = 2$ | **36.70** | **34.86** | **37.26** |
| $K^s = 3$ | 36.18 | 32.67 | 37.21 |
| $K^s = 4$ | 35.92 | 32.06 | 37.07 |

(d) Analysis of fusion strategy

| Model | Full | Rare | Non-Rare |
|---|---|---|---|
| Baseline | 35.72 | 32.20 | 36.56 |
| + *Homo.* | 36.23 | 32.40 | 37.20 |
| + *Hetero.* | **36.70** | **34.86** | **37.26** |

(e) Analysis of geometric group layer

| Group Layer | Full | Rare | Non-Rare |
|---|---|---|---|
| $L^g = 1$ | **36.70** | **34.86** | **37.26** |
| $L^g = 2$ | 36.47 | 31.96 | 37.81 |
| $L^g = 3$ | 35.64 | 31.20 | 37.00 |
| $L^g = 4$ | 36.17 | 32.72 | 37.20 |

(f) Analysis of semantic group layer

| Group Layer | Full | Rare | Non-Rare |
|---|---|---|---|
| $L^s = 1$ | 36.13 | 31.58 | 37.49 |
| $L^s = 2$ | 36.53 | 32.20 | 37.82 |
| $L^s = 3$ | **36.70** | **34.86** | **37.26** |
| $L^s = 4$ | 36.13 | 31.53 | 37.51 |

**Analysis of Group Size.** We evaluate the impact of the geometric group size $K^g$ and semantic group size $K^s$ in Table 4 (b) and (c). Our design performs independent group construction at each decoder layer, allowing entities and interactions to exchange information with different neighbors across layers. As shown in the table, the performance peaks at $K^g = 4$ and drops as $K^g$ increases, suggesting that oversized geometric groups introduce noise from less relevant neighbors. In contrast, the model performs best at $K^s = 2$, and both larger and smaller $K^s$ degrade performance, implying only highly relevant semantic cues are beneficial for interaction prediction. Notably, since groups are constructed independently per layer, the geometric and semantic group sizes across the three-layer decoder range from 4-10 and 2-4, respectively, under the optimal setup. This aligns with real-world scenarios: over 94% of samples in V-COCO [18] and 91% in HICO-DET [2] involve no more than 10 entities, and even large groups are dominated by a few key participants (only around 4) [82].

**Homo. *vs*. Hetero. Geometric Group.** We make a comparison between homogeneous and heterogeneous paradigms for geometric groups in Table 4 (d). The heterogeneous paradigm models humans and objects as distinct node types with exclusive intra-class (human-human/object-object) message passing. In contrast, the homogeneous paradigm treats all entities uniformly, allowing unrestricted cross-entity communication. The heterogeneous design achieves higher performance, surpassing the homogeneous counterpart by **0.47/2.46/0.06** mAP. This disparity suggests that integrating humans and objects into a group may dilute relevant context and hinder the specialized information exchange.

(a) human work on computer
human sit chair

(b) human ride elephant

(c) human kick ball

(d) human carry suitcase
human walk

(e) human hold baseball bat
human hit ball

(f) human work on computer
human hold mouse

(g) human sit car
human talk on phone

(h) human hold umbrella
human carry bag

(i) human sit chair
human hold phone

(j) human ride snowboard

(k) human hit ball
human look at ball

(l) human jump
human look at ball

Figure 3: **Visualization of GroupHOI results** on V-COCO [18] `test`. The first two rows represent samples where all interactions are successfully detected, while the third row corresponds to samples with missed interactions. Detected interactions are marked in Green, while missed interactions and objects are in Red.

**Analysis of Group Layer.** Table 4 (e) and (f) present the evaluation of geometric group layer $L^g$ and semantic group layer $L^s$. We observe that increasing $L^g$ does not lead to consistent improvement. While the performance improves as $L^s$ increases from 1 to 3, after which the gains plateau, indicating that excessive local context aggregation brings diminishing returns.

**Comparison of Model Efficiency.** Table 5 compares the model scalability in terms of the number of Parameters (Params), Floating Point Operations (FLOPs), and Frames Per Second (FPS). Although GroupHOI maintains a comparable parameter count and experiences only a marginal reduction in inference speed compared to HOICLIP [4], it achieves significantly better performance, outperforming HOICLIP by **2.11** mAP on HICO-DET [2] (see Table 1). Compared to ViPLO [83], GroupHOI achieves superior performance (**+1.75** mAP) while requiring fewer parameters and less inference time, underscoring its efficiency. A detailed comparison is available in Table S2 in Appendix.

Table 5: Comparison of **model efficiency**.

| Method | Params↓ | FLOPs↓ | FPS↑ |
|---|---|---|---|
| PPDM [31] [CVPR20] | 194.9M | 121.63G | 15.28 |
| GEN-VLKT [3] [CVPR22] | 41.9M | 60.04G | 26.18 |
| HOICLIP [4] [CVPR23] | 66.1M | 104.68G | 19.57 |
| ViPLO [83] [CVPR23] | 118.2M | 41.35G | 14.89 |
| GroupHOI (ours) | 79.2M | 83.67G | 16.42 |

### 4.4 Qualitative Results

Fig. 3 illustrates the qualitative results of GroupHOI on V-COCO [18] `test`. As seen, it can robustly localize and predict interactions under challenging conditions. For instance, our method generalizes well to interactions with little training data like *riding elephant* in Fig. 3(b), consistent with its superior rare-set performance (Table 1). As shown in Fig. 3(c-h), GroupHOI also handles complex scenes with multiple humans and objects, benefiting from effective intra-group information propagation. The third row presents failure cases, mainly due to: **i)** severe occlusion causing missed detections, *e.g.*, the failure in detecting *human hold phone* (Fig. 3(i)) and *human ride skateboard* (Fig. 3(j)). **ii)** Ambiguous interactions arising from insufficient spatiotemporal information, such as difficulty in recognizing gaze direction (Fig. 3(k)). **iii)** Lack of domain-specific knowledge, exemplified by the misclassification of *looking at ball* as *kicking ball* in (Fig. 3(l)), which is caused by lacking knowledge of basketball, *i.e.*, players typically do not use their feet to kick the ball during games. These

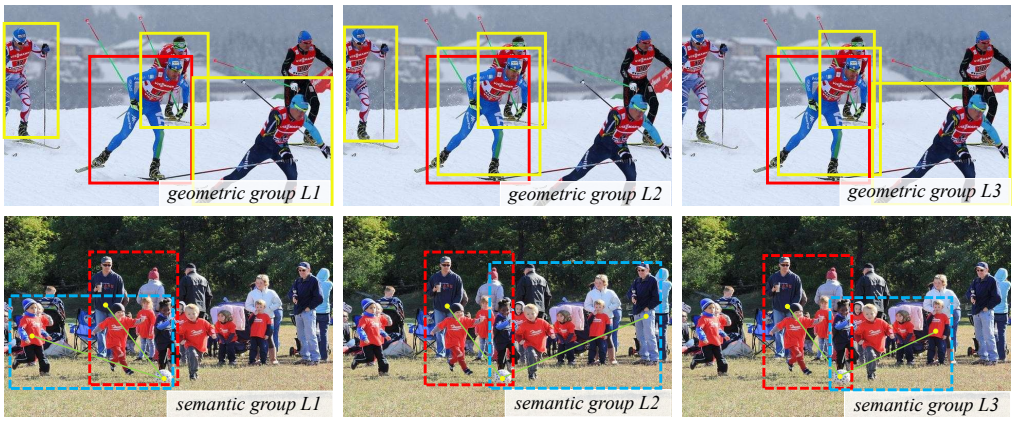


Figure 4: **Visualization of groups** on V-COCO [18] `test`. L1, L2 and L3 represent the first, second and last layer of instance or interaction decoder. The center of the geometric and semantic groups is mark in Red (§4.5).

limitations could potentially be addressed by developing spatiotemporal reasoning modules based on video-level datasets [84] or integrating knowledge via pre-trained large language models [40].

### 4.5 Visualization of Groups

Fig. 4 shows examples of geometric and semantic groups across decoder layers on V-COCO [18] `test`. In the first row, two main geometric group patterns emerge: **i)** multiple proposals targeting to the same human/object, enabling feature completion; **ii)** adjacent distinct proposals that interact closely to show mutual influence. Moreover, groups may also include unannotated entities, revealing GroupHOI's ability to exploit implicit contextual relations. When grouping by semantic similarity (the second row of Fig. 4), the grouping patterns can also be observed, *i.e.*, distinct individuals performing the same interaction. In summary, our method demonstrates the capability to automatically uncover latent patterns in complex scenarios, thereby enhancing the model's holistic scene comprehension.

## 5 Discussion

**Future Direction.** Current HOI benchmarks involve limited entities within small fields of view, leading to global relational modeling in the mainstream HOI-DET [18] methods. However, when applied to larger scenarios (*e.g.*, gigapixel-level crowd images [61]), this paradigm leads to high computational cost and information redundancy. A practical solution is to confine relational modeling to local regions, making the principles proposed in this paper highly applicable to real-world settings.

**Limitation.** A limitation of our method is its focus on interaction reasoning without integrating the proposed mechanisms into the object detection branch. We think this direction intriguing, yet it lies beyond the scope of the present study. Moreover, like other HOI-DET [18] models, GroupHOI is trained with limited label diversity, posing challenges for generalization to in-the-wild scenarios.

## 6 Conclusion

We present GoupHOI, a framework builds upon the idea of reorganizing the unordered in the visual scenes by exploring their inherent grouping patterns. By revisiting HOI-DET [18] task from a group perspective, we formulate two visual attraction principles, *i.e.*, *geometric proximity* and *semantic similarity*, to explain group dynamics. These principles are instantiated via two paradigms: **i)** learning entities as geometric groups, and **ii)** learning interactions as semantic groups. By introducing marginal computational overhead, GroupHOI advances state-of-the-art methods by solid margins and sets new SOTAs for HOI-DET and NVI-DET [20] task, which verifies its superiority.

**Acknowledgement.** This work was supported by National Natural Science Foundation of China (No. 62372405), Fundamental Research Funds for the Central Universities (226-2025-00057), Zhejiang Provincial Natural Science Foundation of China (No. LD25F020001), and CIE-Tencent Robotics X Rhino-Bird Focused Research Program.

## References


[1] Georgia Gkioxari, Ross Girshick, Piotr Dollár, and Kaiming He. Detecting and recognizing human-object interactions. In *CVPR*, 2018. 1, 2

[2] Yu-Wei Chao, Yunfan Liu, Xieyang Liu, Huayi Zeng, and Jia Deng. Learning to detect human-object interactions. In *WACV*, 2018. 1, 2, 6, 7, 8, 9, 22, 23

[3] Yue Liao, Aixi Zhang, Miao Lu, Yongliang Wang, Xiaobo Li, and Si Liu. Gen-vlkt: Simplify association and enhance interaction understanding for hoi detection. In *CVPR*, 2022. 1, 3, 5, 6, 7, 8, 9, 23

[4] Shan Ning, Longtian Qiu, Yongfei Liu, and Xuming He. Hoiclip: Efficient knowledge transfer for hoi detection with vision-language models. In *CVPR*, 2023. 1, 3, 5, 6, 7, 9, 22, 23

[5] Shaoqing Ren, Kaiming He, Ross Girshick, and Jian Sun. Faster r-cnn: Towards real-time object detection with region proposal networks. In *NeurIPS*, 2015. 1, 3

[6] Nicolas Carion, Francisco Massa, Gabriel Synnaeve, Nicolas Usunier, Alexander Kirillov, and Sergey Zagoruyko. End-to-end object detection with transformers. In *ECCV*, 2020. 1, 3, 6

[7] Ding Jia, Yuhui Yuan, Haodi He, Xiaopei Wu, Haojun Yu, Weihong Lin, Lei Sun, Chao Zhang, and Han Hu. Detrs with hybrid matching. In *CVPR*, 2023. 1

[8] Alec Radford, Jong Wook Kim, Chris Hallacy, Aditya Ramesh, Gabriel Goh, Sandhini Agarwal, Girish Sastry, Amanda Askell, Pamela Mishkin, Jack Clark, et al. Learning transferable visual models from natural language supervision. In *ICML*, 2021. 1, 3, 6, 22

[9] Junnan Li, Dongxu Li, Caiming Xiong, and Steven Hoi. Blip: Bootstrapping language-image pre-training for unified vision-language understanding and generation. In *ICML*, 2022. 1, 3, 6

[10] Weibo Jiang, Weihong Ren, Jiandong Tian, Liangqiong Qu, Zhiyong Wang, and Honghai Liu. Exploring self-and cross-triplet correlations for human-object interaction detection. In *AAAI*, 2024. 1, 3

[11] Siyuan Qi, Wenguan Wang, Baoxiong Jia, Jianbing Shen, and Song-Chun Zhu. Learning human-object interactions by graph parsing neural networks. In *ECCV*, 2018. 1, 3, 4

[12] Oytun Ulutan, ASM Iftekhar, and Bangalore S Manjunath. Vsgnet: Spatial attention network for detecting human object interactions using graph convolutions. In *CVPR*, 2020. 1, 4

[13] Hai Wang, Wei-shi Zheng, and Ling Yingbiao. Contextual heterogeneous graph network for human-object interaction detection. In *ECCV*, 2020. 1, 3, 4

[14] Ravin Alaei and Nicholas O Rule. Accuracy of perceiving social attributes. *The social psychology of perceiving others accurately*, 2016. 2

[15] Michael Tomasello. *Why we cooperate*. MIT press, 2009. 2

[16] Willis D Ellis. *A source book of Gestalt psychology*. Routledge, 2013. 2, 4, 5

[17] Aixi Zhang, Yue Liao, Si Liu, Miao Lu, Yongliang Wang, Chen Gao, and Xiaobo Li. Mining the benefits of two-stage and one-stage hoi detection. In *NeurIPS*, 2021. 2, 7, 8, 23

[18] Saurabh Gupta and Jitendra Malik. Visual semantic role labeling. *arXiv preprint arXiv:1505.04474*, 2015. 2, 6, 7, 8, 9, 10, 23, 25

[19] Eastman ZY Wu, Yali Li, Yuan Wang, and Shengjin Wang. Exploring pose-aware human-object interaction via hybrid learning. In *CVPR*, 2024. 2, 3, 6, 7

[20] Jianan Wei, Tianfei Zhou, Yi Yang, and Wenguan Wang. Nonverbal interaction detection. In *ECCV*, 2024. 2, 7, 8, 10

[21] Bo Wan, Desen Zhou, Yongfei Liu, Rongjie Li, and Xuming He. Pose-aware multi-level feature network for human object interaction detection. In *ICCV*, 2019. 2

[22] Chen Gao, Yuliang Zou, and Jia-Bin Huang. ican: Instance-centric attention network for human-object interaction detection. *arXiv preprint arXiv:1808.10437*, 2018. 23

[23] Yong-Lu Li, Siyuan Zhou, Xijie Huang, Liang Xu, Ze Ma, Hao-Shu Fang, Yanfeng Wang, and Cewu Lu. Transferable interactiveness knowledge for human-object interaction detection. In *CVPR*, 2019. 3

[24] Tanmay Gupta, Alexander Schwing, and Derek Hoiem. No-frills human-object interaction detection: Factorization, layout encodings, and training techniques. In *ICCV*, 2019.

[25] Yang Liu, Qingchao Chen, and Andrew Zisserman. Amplifying key cues for human-object-interaction detection. In *ECCV*, 2020. 3

[26] Dong-Jin Kim, Xiao Sun, Jinsoo Choi, Stephen Lin, and In So Kweon. Detecting human-object interactions with action co-occurrence priors. In *ECCV*, 2020.

[27] Tianfei Zhou, Wenguan Wang, Siyuan Qi, Haibin Ling, and Jianbing Shen. Cascaded human-object interaction recognition. In *CVPR*, 2020.

[28] Tianfei Zhou, Siyuan Qi, Wenguan Wang, Jianbing Shen, and Song-Chun Zhu. Cascaded parsing of human-object interaction recognition. *IEEE TPAMI*, 2021. 2

[29] Hao-Shu Fang, Yichen Xie, Dian Shao, and Cewu Lu. Dirv: Dense interaction region voting for end-to-end human-object interaction detection. In *AAAI*, 2021. 3

[30] Xubin Zhong, Xian Qu, Changxing Ding, and Dacheng Tao. Glance and gaze: Inferring action-aware points for one-stage human-object interaction detection. In *CVPR*, 2021. 3

[31] Yue Liao, Si Liu, Fei Wang, Yanjie Chen, Chen Qian, and Jiashi Feng. Ppdm: Parallel point detection and matching for real-time human-object interaction detection. In *CVPR*, 2020. 9, 23

[32] Frederic Z Zhang, Dylan Campbell, and Stephen Gould. Spatially conditioned graphs for detecting human-object interactions. In *ICCV*, 2021. 3, 4, 23

[33] Yong Zhang, Yingwei Pan, Ting Yao, Rui Huang, Tao Mei, and Chang-Wen Chen. Exploring structure-aware transformer over interaction proposals for human-object interaction detection. In *CVPR*, 2022. 3, 6, 7, 23

[34] Desen Zhou, Zhichao Liu, Jian Wang, Leshan Wang, Tao Hu, Errui Ding, and Jingdong Wang. Human-object interaction detection via disentangled transformer. In *CVPR*, 2022.

[35] Bumsoo Kim, Taeho Choi, Jaewoo Kang, and Hyunwoo J Kim. Uniondet: Union-level detector towards real-time human-object interaction detection. In *ECCV*, 2020.

[36] Tiancai Wang, Tong Yang, Martin Danelljan, Fahad Shahbaz Khan, Xiangyu Zhang, and Jian Sun. Learning human-object interaction detection using interaction points. In *CVPR*, 2020.

[37] Cheng Zou, Bohan Wang, Yue Hu, Junqi Liu, Qian Wu, Yu Zhao, Boxun Li, Chenguang Zhang, Chi Zhang, Yichen Wei, et al. End-to-end human object interaction detection with hoi transformer. In *CVPR*, 2021. 23

[38] Liulei Li, Jianan Wei, Wenguan Wang, and Yi Yang. Neural-logic human-object interaction detection. In *NeurIPS*, 2024. 7

[39] Minghan Chen, Guikun Chen, Wenguan Wang, and Yi Yang. Hydra-sgg: Hybrid relation assignment for one-stage scene graph generation. In *ICLR*, 2025. 3

[40] Yichao Cao, Qingfei Tang, Xiu Su, Song Chen, Shan You, Xiaobo Lu, and Chang Xu. Detecting any human-object interaction relationship: Universal hoi detector with spatial prompt learning on foundation models. In *NeurIPS*, 2023. 3, 6, 7, 10

[41] Jie Yang, Bingliang Li, Fengyu Yang, Ailing Zeng, Lei Zhang, and Ruimao Zhang. Boosting human-object interaction detection with text-to-image diffusion model. *arXiv preprint arXiv:2305.12252*, 2023.

[42] Liulei Li, Wenguan Wang, and Yi Yang. Human-object interaction detection collaborated with large relation-driven diffusion models. In *NeurIPS*, 2024.

[43] Jinguo Luo, Weihong Ren, Weibo Jiang, Xi'ai Chen, Qiang Wang, Zhi Han, and Honghai Liu. Discovering syntactic interaction clues for human-object interaction detection. In *CVPR*, 2024.

[44] Guikun Chen, Jin Li, and Wenguan Wang. Scene graph generation with role-playing large language models. In *NeurIPS*, 2024. 3

[45] Robin Rombach, Andreas Blattmann, Dominik Lorenz, Patrick Esser, and Björn Ommer. High-resolution image synthesis with latent diffusion models. In *CVPR*, 2022. 3

[46] Susan Zhang, Stephen Roller, Naman Goyal, Mikel Artetxe, Moya Chen, Shuohui Chen, Christopher Dewan, Mona Diab, Xian Li, Xi Victoria Lin, et al. Opt: Open pre-trained transformer language models. *arXiv preprint arXiv:2205.01068*, 2022. 3

[47] Ross Girshick, Jeff Donahue, Trevor Darrell, and Jitendra Malik. Rich feature hierarchies for accurate object detection and semantic segmentation. In *CVPR*, 2014. 3

[48] Ross Girshick. Fast r-cnn. In *ICCV*, 2015.

[49] Shaoqing Ren, Kaiming He, Ross Girshick, and Jian Sun. Faster r-cnn: Towards real-time object detection with region proposal networks. In *NeurIPS*, 2015. 3

[50] Jianan Li, Xiaodan Liang, Jianshu Li, Yunchao Wei, Tingfa Xu, Jiashi Feng, and Shuicheng Yan. Multistage object detection with group recursive learning. *IEEE TMM*, 2017. 3

[51] Wonmin Byeon, Thomas M Breuel, Federico Raue, and Marcus Liwicki. Scene labeling with lstm recurrent neural networks. In *CVPR*, 2015. 3

[52] Tao He, Lianli Gao, Jingkuan Song, and Yuan-Fang Li. Exploiting scene graphs for human-object interaction detection. In *ICCV*, 2021. 3

[53] Penghao Zhou and Mingmin Chi. Relation parsing neural network for human-object interaction detection. In *ICCV*, 2019.

[54] Chen Gao, Jiarui Xu, Yuliang Zou, and Jia-Bin Huang. Drg: Dual relation graph for human-object interaction detection. In *ECCV*, 2020. 4, 23

[55] Lifeng Fan, Wenguan Wang, Siyuan Huang, Xinyu Tang, and Song-Chun Zhu. Understanding human gaze communication by spatio-temporal graph reasoning. In *ICCV*, 2019.

[56] Mu Chen, Liulei Li, Wenguan Wang, and Yi Yang. Diffvsgg: Diffusion-driven online video scene graph generation. In *CVPR*, 2025. 3

[57] Chenxin Xu, Maosen Li, Zhenyang Ni, Ya Zhang, and Siheng Chen. Groupnet: Multiscale hypergraph neural networks for trajectory prediction with relational reasoning. In *CVPR*, 2022. 3

[58] Buzhen Huang, Jingyi Ju, Zhihao Li, and Yangang Wang. Reconstructing groups of people with hypergraph relational reasoning. In *ICCV*, 2023. 3

[59] Jing Shao, Chen Change Loy, and Xiaogang Wang. Scene-independent group profiling in crowd. In *CVPR*, 2014. 3

[60] Loris Bazzani, Marco Cristani, and Vittorio Murino. Decentralized particle filter for joint individual-group tracking. In *CVPR*, 2012. 3

[61] Xueyang Wang, Xiya Zhang, Yinheng Zhu, Yuchen Guo, Xiaoyun Yuan, Liuyu Xiang, Zerun Wang, Guiguang Ding, David Brady, Qionghai Dai, et al. Panda: A gigapixel-level human-centric video dataset. In *CVPR*, 2020. 3, 10

[62] Stefano Pellegrini, Andreas Ess, and Luc Van Gool. Improving data association by joint modeling of pedestrian trajectories and groupings. In *ECCV*, 2010. 3

[63] Kota Yamaguchi, Alexander C Berg, Luis E Ortiz, and Tamara L Berg. Who are you with and where are you going? In *CVPR*, 2011.

[64] Agrim Gupta, Justin Johnson, Li Fei-Fei, Silvio Savarese, and Alexandre Alahi. Social gan: Socially acceptable trajectories with generative adversarial networks. In *CVPR*, 2018. 3

[65] Jianchao Wu, Limin Wang, Li Wang, Jie Guo, and Gangshan Wu. Learning actor relation graphs for group activity recognition. In *CVPR*, 2019. 3

[66] Rui Yan, Lingxi Xie, Jinhui Tang, Xiangbo Shu, and Qi Tian. Social adaptive module for weakly-supervised group activity recognition. In *ECCV*, 2020. 3

[67] Masato Tamura, Hiroki Ohashi, and Tomoaki Yoshinaga. Qpic: Query-based pairwise human-object interaction detection with image-wide contextual information. In *CVPR*, 2021. 3, 5, 7, 8, 23

[68] Ting Lei, Shaofeng Yin, Yuxin Peng, and Yang Liu. Exploring conditional multi-modal prompts for zero-shot hoi detection. In *ECCV*, 2024. 3, 6, 7

[69] Bumsoo Kim, Junhyun Lee, Jaewoo Kan, Eun-Sol Kim, and Hyunwoo J Kim. Hotr: End-to-end human-object interaction detection with transformers. In *CVPR*, 2021. 3, 7, 23

[70] Tanqiu Qiao, Qianhui Men, Frederick WB Li, Yoshiki Kubotani, Shigeo Morishima, and Hubert PH Shum. Geometric features informed multi-person human-object interaction recognition in videos. In *ECCV*, 2022. 4

[71] Frederic Z. Zhang, Yuhui Yuan, Dylan Campbell, Zhuoyao Zhong, and Stephen Gould. Exploring predicate visual context in detecting human–object interactions. In *ICCV*, 2023. 5, 7

[72] Kaiming He, Xiangyu Zhang, Shaoqing Ren, and Jian Sun. Deep residual learning for image recognition. In *CVPR*, 2016. 5

[73] Tsung-Yi Lin, Michael Maire, Serge Belongie, James Hays, Pietro Perona, Deva Ramanan, Piotr Dollár, and C Lawrence Zitnick. Microsoft coco: Common objects in context. In *ECCV*, 2014. 6

[74] Ilya Loshchilov and Frank Hutter. Decoupled weight decay regularization. *arXiv preprint arXiv:1711.05101*, 2017. 6

[75] Shuman Fang, Shuai Liu, Jie Li, Guannan Jiang, Xianming Lin, and Rongrong Ji. Improving human-object interaction detection via virtual image learning. In *ACM MM*, 2023. 6, 7

[76] Chi Xie, Fangao Zeng, Yue Hu, Shuang Liang, and Yichen Wei. Category query learning for human-object interaction classification. In *CVPR*, 2023. 6, 7

[77] Bumsoo Kim, Jonghwan Mun, Kyoung-Woon On, Minchul Shin, Junhyun Lee, and Eun-Sol Kim. Mstr: Multi-scale transformer for end-to-end human-object interaction detection. In *CVPR*, 2022. 7

[78] Xian Qu, Changxing Ding, Xingao Li, Xubin Zhong, and Dacheng Tao. Distillation using oracle queries for transformer-based human-object interaction detection. In *CVPR*, 2022. 7

[79] Ting Lei, Fabian Caba, Qingchao Chen, Hailin Jin, Yuxin Peng, and Yang Liu. Efficient adaptive human-object interaction detection with concept-guided memory. In *ICCV*, 2023. 7

[80] Lijun Zhang, Wei Suo, Peng Wang, and Yanning Zhang. A plug-and-play method for rare human-object interactions detection by bridging domain gap. In *ACM MM*, 2024. 7

[81] Long Zhao, Liangzhe Yuan, Boqing Gong, Yin Cui, Florian Schroff, Ming-Hsuan Yang, Hartwig Adam, and Ting Liu. Unified visual relationship detection with vision and language models. In *ICCV*, 2023. 7

[82] Nicolas Fay, Simon Garrod, and Jean Carletta. Group discussion as interactive dialogue or as serial monologue: The influence of group size. *Psychological science*, 2000. 8

[83] Jeeseung Park, Jin-Woo Park, and Jong-Seok Lee. Viplo: Vision transformer based pose-conditioned self-loop graph for human-object interaction detection. In *CVPR*, 2023. 9, 23

[84] Hema S Koppula and Ashutosh Saxena. Anticipating human activities using object affordances for reactive robotic response. *IEEE TPAMI*, 2015. 10

[85] Tal Ridnik, Emanuel Ben-Baruch, Nadav Zamir, Asaf Noy, Itamar Friedman, Matan Protter, and Lihi Zelnik-Manor. Asymmetric loss for multi-label classification. In *ICCV*, 2021. 22

[86] Mingfei Chen, Yue Liao, Si Liu, Zhiyuan Chen, Fei Wang, and Chen Qian. Reformulating hoi detection as adaptive set prediction. In *CVPR*, 2021. 23

[87] Yunyao Mao, Jiajun Deng, Wengang Zhou, Li Li, Yao Fang, and Houqiang Li. Clip4hoi: Towards adapting clip for practical zero-shot hoi detection. In *NeurIPS*, 2023. 23

## NeurIPS Paper Checklist

1. **Claims**

   Question: Do the main claims made in the abstract and introduction accurately reflect the paper's contributions and scope?

   Answer: [Yes]

   Justification: The abstract and introduction make claims which accurately reflect the paper's contributions and scope.

   Guidelines:

   - The answer NA means that the abstract and introduction do not include the claims made in the paper.
   - The abstract and/or introduction should clearly state the claims made, including the contributions made in the paper and important assumptions and limitations. A No or NA answer to this question will not be perceived well by the reviewers.
   - The claims made should match theoretical and experimental results, and reflect how much the results can be expected to generalize to other settings.
   - It is fine to include aspirational goals as motivation as long as it is clear that these goals are not attained by the paper.

2. **Limitations**

   Question: Does the paper discuss the limitations of the work performed by the authors?

   Answer: [Yes]

   Justification: The main limitations are discussed in §5.

   Guidelines:

   - The answer NA means that the paper has no limitation while the answer No means that the paper has limitations, but those are not discussed in the paper.
   - The authors are encouraged to create a separate "Limitations" section in their paper.
   - The paper should point out any strong assumptions and how robust the results are to violations of these assumptions (e.g., independence assumptions, noiseless settings, model well-specification, asymptotic approximations only holding locally). The authors should reflect on how these assumptions might be violated in practice and what the implications would be.
   - The authors should reflect on the scope of the claims made, e.g., if the approach was only tested on a few datasets or with a few runs. In general, empirical results often depend on implicit assumptions, which should be articulated.
   - The authors should reflect on the factors that influence the performance of the approach. For example, a facial recognition algorithm may perform poorly when image resolution is low or images are taken in low lighting. Or a speech-to-text system might not be used reliably to provide closed captions for online lectures because it fails to handle technical jargon.
   - The authors should discuss the computational efficiency of the proposed algorithms and how they scale with dataset size.
   - If applicable, the authors should discuss possible limitations of their approach to address problems of privacy and fairness.
   - While the authors might fear that complete honesty about limitations might be used by reviewers as grounds for rejection, a worse outcome might be that reviewers discover limitations that aren't acknowledged in the paper. The authors should use their best judgment and recognize that individual actions in favor of transparency play an important role in developing norms that preserve the integrity of the community. Reviewers will be specifically instructed to not penalize honesty concerning limitations.

3. **Theory assumptions and proofs**

   Question: For each theoretical result, does the paper provide the full set of assumptions and a complete (and correct) proof?

   Answer: [NA]

Justification: There is no theoretical result.

Guidelines:

- The answer NA means that the paper does not include theoretical results.
- All the theorems, formulas, and proofs in the paper should be numbered and cross-referenced.
- All assumptions should be clearly stated or referenced in the statement of any theorems.
- The proofs can either appear in the main paper or the supplemental material, but if they appear in the supplemental material, the authors are encouraged to provide a short proof sketch to provide intuition.
- Inversely, any informal proof provided in the core of the paper should be complemented by formal proofs provided in appendix or supplemental material.
- Theorems and Lemmas that the proof relies upon should be properly referenced.

4. **Experimental result reproducibility**

   Question: Does the paper fully disclose all the information needed to reproduce the main experimental results of the paper to the extent that it affects the main claims and/or conclusions of the paper (regardless of whether the code and data are provided or not)?

   Answer: [Yes]

   Justification: The implementation details have been provided in §3.5.

   Guidelines:

   - The answer NA means that the paper does not include experiments.
   - If the paper includes experiments, a No answer to this question will not be perceived well by the reviewers: Making the paper reproducible is important, regardless of whether the code and data are provided or not.
   - If the contribution is a dataset and/or model, the authors should describe the steps taken to make their results reproducible or verifiable.
   - Depending on the contribution, reproducibility can be accomplished in various ways. For example, if the contribution is a novel architecture, describing the architecture fully might suffice, or if the contribution is a specific model and empirical evaluation, it may be necessary to either make it possible for others to replicate the model with the same dataset, or provide access to the model. In general. releasing code and data is often one good way to accomplish this, but reproducibility can also be provided via detailed instructions for how to replicate the results, access to a hosted model (e.g., in the case of a large language model), releasing of a model checkpoint, or other means that are appropriate to the research performed.
   - While NeurIPS does not require releasing code, the conference does require all submissions to provide some reasonable avenue for reproducibility, which may depend on the nature of the contribution. For example
     (a) If the contribution is primarily a new algorithm, the paper should make it clear how to reproduce that algorithm.
     (b) If the contribution is primarily a new model architecture, the paper should describe the architecture clearly and fully.
     (c) If the contribution is a new model (e.g., a large language model), then there should either be a way to access this model for reproducing the results or a way to reproduce the model (e.g., with an open-source dataset or instructions for how to construct the dataset).
     (d) We recognize that reproducibility may be tricky in some cases, in which case authors are welcome to describe the particular way they provide for reproducibility. In the case of closed-source models, it may be that access to the model is limited in some way (e.g., to registered users), but it should be possible for other researchers to have some path to reproducing or verifying the results.

5. **Open access to data and code**

   Question: Does the paper provide open access to the data and code, with sufficient instructions to faithfully reproduce the main experimental results, as described in supplemental material?

Answer: [Yes]

Justification: Code is available at https://github.com/JiajunHong1/GroupHOI.

Guidelines:

- The answer NA means that paper does not include experiments requiring code.
- Please see the NeurIPS code and data submission guidelines (https://nips.cc/public/guides/CodeSubmissionPolicy) for more details.
- While we encourage the release of code and data, we understand that this might not be possible, so "No" is an acceptable answer. Papers cannot be rejected simply for not including code, unless this is central to the contribution (e.g., for a new open-source benchmark).
- The instructions should contain the exact command and environment needed to run to reproduce the results. See the NeurIPS code and data submission guidelines (https://nips.cc/public/guides/CodeSubmissionPolicy) for more details.
- The authors should provide instructions on data access and preparation, including how to access the raw data, preprocessed data, intermediate data, and generated data, etc.
- The authors should provide scripts to reproduce all experimental results for the new proposed method and baselines. If only a subset of experiments are reproducible, they should state which ones are omitted from the script and why.
- At submission time, to preserve anonymity, the authors should release anonymized versions (if applicable).
- Providing as much information as possible in supplemental material (appended to the paper) is recommended, but including URLs to data and code is permitted.

6. **Experimental setting/details**

   Question: Does the paper specify all the training and test details (e.g., data splits, hyperparameters, how they were chosen, type of optimizer, etc.) necessary to understand the results?

   Answer: [Yes]

   Justification: The experimental setup, including data splits, training and testing detailed, are provided in §4.1.

   Guidelines:

   - The answer NA means that the paper does not include experiments.
   - The experimental setting should be presented in the core of the paper to a level of detail that is necessary to appreciate the results and make sense of them.
   - The full details can be provided either with the code, in appendix, or as supplemental material.

7. **Experiment statistical significance**

   Question: Does the paper report error bars suitably and correctly defined or other appropriate information about the statistical significance of the experiments?

   Answer: [No]

   Justification: The prior work included into comparison does not provide error bar. It could be too expensive and time-consuming to run the experiments on large-scale datasets for multiple times

   Guidelines:

   - The answer NA means that the paper does not include experiments.
   - The authors should answer "Yes" if the results are accompanied by error bars, confidence intervals, or statistical significance tests, at least for the experiments that support the main claims of the paper.
   - The factors of variability that the error bars are capturing should be clearly stated (for example, train/test split, initialization, random drawing of some parameter, or overall run with given experimental conditions).
   - The method for calculating the error bars should be explained (closed form formula, call to a library function, bootstrap, etc.)

- The assumptions made should be given (e.g., Normally distributed errors).
- It should be clear whether the error bar is the standard deviation or the standard error of the mean.
- It is OK to report 1-sigma error bars, but one should state it. The authors should preferably report a 2-sigma error bar than state that they have a 96% CI, if the hypothesis of Normality of errors is not verified.
- For asymmetric distributions, the authors should be careful not to show in tables or figures symmetric error bars that would yield results that are out of range (e.g. negative error rates).
- If error bars are reported in tables or plots, The authors should explain in the text how they were calculated and reference the corresponding figures or tables in the text.

8. **Experiments compute resources**

   Question: For each experiment, does the paper provide sufficient information on the computer resources (type of compute workers, memory, time of execution) needed to reproduce the experiments?

   Answer: [Yes]

   Justification: The computer resources are described in §4.1.

   Guidelines:

   - The answer NA means that the paper does not include experiments.
   - The paper should indicate the type of compute workers CPU or GPU, internal cluster, or cloud provider, including relevant memory and storage.
   - The paper should provide the amount of compute required for each of the individual experimental runs as well as estimate the total compute.
   - The paper should disclose whether the full research project required more compute than the experiments reported in the paper (e.g., preliminary or failed experiments that didn't make it into the paper).

9. **Code of ethics**

   Question: Does the research conducted in the paper conform, in every respect, with the NeurIPS Code of Ethics https://neurips.cc/public/EthicsGuidelines?

   Answer: [Yes]

   Justification: This work conforms the NeurIPS Code of Ethics.

   Guidelines:

   - The answer NA means that the authors have not reviewed the NeurIPS Code of Ethics.
   - If the authors answer No, they should explain the special circumstances that require a deviation from the Code of Ethics.
   - The authors should make sure to preserve anonymity (e.g., if there is a special consideration due to laws or regulations in their jurisdiction).

10. **Broader impacts**

    Question: Does the paper discuss both potential positive societal impacts and negative societal impacts of the work performed?

    Answer: [Yes]

    Justification: The border impacts is provided in Appendix.

    Guidelines:

    - The answer NA means that there is no societal impact of the work performed.
    - If the authors answer NA or No, they should explain why their work has no societal impact or why the paper does not address societal impact.
    - Examples of negative societal impacts include potential malicious or unintended uses (e.g., disinformation, generating fake profiles, surveillance), fairness considerations (e.g., deployment of technologies that could make decisions that unfairly impact specific groups), privacy considerations, and security considerations.

- The conference expects that many papers will be foundational research and not tied to particular applications, let alone deployments. However, if there is a direct path to any negative applications, the authors should point it out. For example, it is legitimate to point out that an improvement in the quality of generative models could be used to generate deepfakes for disinformation. On the other hand, it is not needed to point out that a generic algorithm for optimizing neural networks could enable people to train models that generate Deepfakes faster.
- The authors should consider possible harms that could arise when the technology is being used as intended and functioning correctly, harms that could arise when the technology is being used as intended but gives incorrect results, and harms following from (intentional or unintentional) misuse of the technology.
- If there are negative societal impacts, the authors could also discuss possible mitigation strategies (e.g., gated release of models, providing defenses in addition to attacks, mechanisms for monitoring misuse, mechanisms to monitor how a system learns from feedback over time, improving the efficiency and accessibility of ML).

11. **Safeguards**

    Question: Does the paper describe safeguards that have been put in place for responsible release of data or models that have a high risk for misuse (e.g., pretrained language models, image generators, or scraped datasets)?

    Answer: [NA]

    Justification: The proposed method uses pre-trained models. This proposed methods is safe under the safeguards of adopted pre-trained models.

    Guidelines:

    - The answer NA means that the paper poses no such risks.
    - Released models that have a high risk for misuse or dual-use should be released with necessary safeguards to allow for controlled use of the model, for example by requiring that users adhere to usage guidelines or restrictions to access the model or implementing safety filters.
    - Datasets that have been scraped from the Internet could pose safety risks. The authors should describe how they avoided releasing unsafe images.
    - We recognize that providing effective safeguards is challenging, and many papers do not require this, but we encourage authors to take this into account and make a best faith effort.

12. **Licenses for existing assets**

    Question: Are the creators or original owners of assets (e.g., code, data, models), used in the paper, properly credited and are the license and terms of use explicitly mentioned and properly respected?

    Answer: [Yes]

    Justification: V-COCO dataset is released under the MIT license. HICO-DET dataset is released under the CC0: Public Domain license. The weight of DETR is released under Apache 2.0 license.

    Guidelines:

    - The answer NA means that the paper does not use existing assets.
    - The authors should cite the original paper that produced the code package or dataset.
    - The authors should state which version of the asset is used and, if possible, include a URL.
    - The name of the license (e.g., CC-BY 4.0) should be included for each asset.
    - For scraped data from a particular source (e.g., website), the copyright and terms of service of that source should be provided.
    - If assets are released, the license, copyright information, and terms of use in the package should be provided. For popular datasets, `paperswithcode.com/datasets` has curated licenses for some datasets. Their licensing guide can help determine the license of a dataset.

- For existing datasets that are re-packaged, both the original license and the license of the derived asset (if it has changed) should be provided.
- If this information is not available online, the authors are encouraged to reach out to the asset's creators.

13. **New assets**

    Question: Are new assets introduced in the paper well documented and is the documentation provided alongside the assets?

    Answer: [Yes]

    Justification: We will release our code base with README file.

    Guidelines:

    - The answer NA means that the paper does not release new assets.
    - Researchers should communicate the details of the dataset/code/model as part of their submissions via structured templates. This includes details about training, license, limitations, etc.
    - The paper should discuss whether and how consent was obtained from people whose asset is used.
    - At submission time, remember to anonymize your assets (if applicable). You can either create an anonymized URL or include an anonymized zip file.

14. **Crowdsourcing and research with human subjects**

    Question: For crowdsourcing experiments and research with human subjects, does the paper include the full text of instructions given to participants and screenshots, if applicable, as well as details about compensation (if any)?

    Answer: [NA]

    Justification: There is no research with human subjects in this work.

    Guidelines:

    - The answer NA means that the paper does not involve crowdsourcing nor research with human subjects.
    - Including this information in the supplemental material is fine, but if the main contribution of the paper involves human subjects, then as much detail as possible should be included in the main paper.
    - According to the NeurIPS Code of Ethics, workers involved in data collection, curation, or other labor should be paid at least the minimum wage in the country of the data collector.

15. **Institutional review board (IRB) approvals or equivalent for research with human subjects**

    Question: Does the paper describe potential risks incurred by study participants, whether such risks were disclosed to the subjects, and whether Institutional Review Board (IRB) approvals (or an equivalent approval/review based on the requirements of your country or institution) were obtained?

    Answer: [NA]

    Justification: There is no research with human subjects in this work.

    Guidelines:

    - The answer NA means that the paper does not involve crowdsourcing nor research with human subjects.
    - Depending on the country in which research is conducted, IRB approval (or equivalent) may be required for any human subjects research. If you obtained IRB approval, you should clearly state this in the paper.
    - We recognize that the procedures for this may vary significantly between institutions and locations, and we expect authors to adhere to the NeurIPS Code of Ethics and the guidelines for their institution.
    - For initial submissions, do not include any information that would break anonymity (if applicable), such as the institution conducting the review.

16. **Declaration of LLM usage**

Question: Does the paper describe the usage of LLMs if it is an important, original, or non-standard component of the core methods in this research? Note that if the LLM is used only for writing, editing, or formatting purposes and does not impact the core methodology, scientific rigorousness, or originality of the research, declaration is not required.

Answer: [Yes]

Justification: LLMs employed in this work are illustrated in §3.5.

Guidelines:

- The answer NA means that the core method development in this research does not involve LLMs as any important, original, or non-standard components.
- Please refer to our LLM policy (https://neurips.cc/Conferences/2025/LLM) for what should or should not be described.

## Summary of the Appendix

For a better understanding of the main paper, we provide additional details in this supplementary material, which is organized as follows:

- §A provides more implementation details of GroupHOI.
- §B offers more qualitative results.
- §C provides more experimental results.
- §D presents the pseudo code of GroupHOI.
- §E discusses the societal impact of this work.

## A More Implementation Details

We follow HOICLIP [4] in converting HOI triplets and object labels into textual descriptions to generate CLIP [8] text embeddings. Specifically, each HOI triplet <human, verb, object> is converted into a sentence like "A photo of a person [verb-ing] a/an [object]". For "no-interaction" instances, we use "A photo of a person and a/an [object]", and object labels are converted into "A photo of a/an [object]". These textual descriptions are then processed by the pre-trained CLIP text encoder to obtain corresponding embeddings, which initialize the weights of the interaction classifier $\mathcal{C}^a$ and object classifier $\mathcal{C}^o$. During training, these classifiers are fine-tuned with a small learning rate to adapt to the specific dataset. We employ the pre-trained CLIP visual encoder to extract visual features $\boldsymbol{V}_{clip}$. These features, along with our encoded features $\boldsymbol{V}_e$, are independently processed by separate interaction decoders. The resulting outputs are then fused to facilitate the final reasoning. We also introduce two key modifications based on HOICLIP [4]. **First**, to address the dimensional mismatch between positional embeddings (256) and the interaction decoder (768), we expand the positional embeddings by stacking them three times. **Second**, we replace the Focal Loss with Asymmetric Loss [85] to better handle the long-tail distribution of HOI categories.

## B More Qualitative Results

We further provide qualitative examples of our approach in Fig. S1. These results highlight GroupHOI's robust performance in HOI detection across various scenes. Notably, our model effectively captures complex interaction patterns in scenarios involving group activities such as team sports (*e.g.*, soccer or tennis). This capability enhances interaction prediction with mutual communication. We also present several failure examples of our model, primarily due to missed object detection, as seen in Fig. S1(c). Additionally, our model encounters challenges when dealing with highly ambiguous relations. For instance, in Fig. S1(s), GroupHOI fails to detect the *look at ball* between the girl at the center and the ball, which is disrupted by her surrounding teammates.

## C More Experiments

**Ablative Experiments.** We evaluate four strategies for measuring geometric proximity between entities, using intersection-over-union (IoU), center distance (CD), and global image features (IF). As shown in Table S1, combining IoU and CD consistently yields the best performance across all splits, indicating that both spatial cues complement each other effectively. In contrast, adding global image features slightly degrades performance, suggesting that they are not essential for proximity estimation.

Table S1: Analysis of geometric proximity measurement on HICO-DET [2] `test`(§C).

| Measurement | Full | Rare | Non-Rare |
|---|---|---|---|
| *IOU only* | 36.02 | 32.19 | 37.16 |
| *CD only* | 36.14 | 33.60 | 36.90 |
| *IOU + CD* | **36.70** | **34.86** | **37.26** |
| *IOU + CD +IF* | 36.21 | 33.45 | 36.97 |

**Efficiency Comparison.** Table S2 presents a comprehensive comparison of the model scalability (*i.e.*, number of Parameters (Params), Floating Point Operations (FLOPs) and Frames Per Second (FPS)) for various HOI detection methods. As shown, GroupHOI achieves significant performance improvements over previous models while maintaining a comparable number of parameters. We also

Table S2: Comparison of efficiency and performance on HICO-DET [2] `test` and V-COCO [18] `test`.

| Method | Backbone | Params↓ | FLOPs↓ | FPS↑ | Default | | | $AP^{S1}_{role}$ | $AP^{S2}_{role}$ |
|---|---|---|---|---|---|---|---|---|---|
| | | | | | Full | Rare | Non-Rare | | |
| iCAN[22][BMVC18] | R50 | 39.8 | - | - | 14.84 | 10.45 | 16.15 | 45.3 | - |
| DRG[54][ECCV20] | R50-FPN | 46.1 | - | - | 19.26 | 17.74 | 19.71 | 51.0 | - |
| PPDM[31][CVPR20] | HG104 | 194.9 | - | - | 21.73 | 13.78 | 24.10 | - | - |
| SCG[32][ICCV21] | R50-FPN | 53.9 | - | - | 31.33 | 24.72 | 33.31 | 54.2 | 60.9 |
| HOTR[69][CVPR21] | R50 | 51.2 | - | - | 25.10 | 17.34 | 27.42 | 55.2 | 64.4 |
| HOITrans[37][CVPR21] | R50 | 41.4 | - | - | 23.46 | 16.91 | 25.41 | 52.9 | - |
| AS-Net[86][CVPR21] | R50 | 52.5 | - | - | 28.87 | 24.25 | 33.14 | 53.9 | - |
| QPIC[67][CVPR21] | R50 | 41.9 | - | - | 29.07 | 21.85 | 31.23 | 58.8 | 61.0 |
| CDN-S[17][NeurIPS21] | R50 | 42.1 | - | - | 31.78 | 27.55 | 33.05 | 62.3 | 64.4 |
| STIP[33][CVPR22] | R50 | 50.4 | - | - | 32.22 | 28.15 | 33.43 | **65.1** | **69.7** |
| GEN-VLKT[3][CVPR22] | R50 | 41.9 | 60.04 | 26.18 | 33.75 | 29.25 | 35.10 | 62.4 | 64.4 |
| HOICLIP[4][CVPR23] | R50 | 66.1 | 104.68 | 19.57 | 34.59 | 31.12 | 35.74 | 63.5 | 64.8 |
| CLIP4HOI[87][NeurIPS23] | R50 | 71.2 | - | - | 35.33 | 33.95 | 35.74 | - | 66.3 |
| ViPLO[83][CVPR23] | ViT-B/32 | 118.2 | - | - | 34.95 | 33.83 | 35.28 | 60.9 | 66.6 |
| GroupHOI (ours) | R50 | 79.2 | 83.67 | 16.42 | **36.70** | **34.86** | **37.26** | 65.0 | 66.0 |

compare FLOPs and FPS with GEN-VLKT [3] and HOICLIP [4]. Despite a marginal reduction in inference speed relative to HOICLIP, GroupHOI has lower FLOPs and yields solid mAP improvements of **2.11/3.74/1.52** in HICO-DET [2], highlighting the effectiveness of our proposed framework.

## D Pseudo Code

The pseudo code for semantic and geometric group are given in Algorithm 1 and Algorithm 2.

**Algorithm 1:** Pseudo-code for Geometric Group in a PyTorch-like style.

```
"""
hs: output human/object embeddings from the instance decoder.
pos_embed: position embeddings for human/object queries.
coords: bounding boxes of humans/objects.
K_g: geometric group size.
"""
def Geometric_Group(hs, pos_embed, coords, K_g):
    # Formulate the spatial feature
    F_p = Cat([Square_distance(coords[:, None], coords[None, :]), IoU(coords[:, None], coords[None, :])])
    # Compute the proximity score
    S = Linear(F_p)
    # Select the topk neighbors
    knn_idx = TopK(S, K_g)

    # Compute the position encodings
    pos_enc = MLP(pos_embed - Gather(pos_embed, knn_idx))
    # Formulate query, key, and value
    q, k, v = Linear(hs), Linear(Gather(hs, knn_idx)), Linear(Gather(hs, knn_idx))
    # Compute dispatch matrix
    G = Softmax(q - k + pos_enc)
    # Aggregate geometric context
    C_g = Linear(G * (v + pos_enc))
    out = hs + C_g

    return out
```

**Algorithm 2:** Pseudo-code for Semantic Group in a PyTorch-like style.

```
"""
hs: interaction embeddings from the interaction decoder.
K_s: semantic group size.
"""
def Semantic_Group(hs, pos_embed, K_s):
    # Compute the similarity score
    S = CosineSimilarity(hs[:, None], hs[:, None])
    # Select the topk neighbors
    knn_idx = TopK(S, K_s)

    # Aggregate semantic context
    C_s = MLP(Max(MLP(hs[:, None], hs[:, None]-Gather(hs, knn_idx)), dim=-1))
    out = hs + C_s

    return out
```

# E Boarder Impact

This work advances the recognition of human-object interactions in complex scenarios, particularly in scenes where small groups of people naturally form, which is a common occurrence in real-world settings. This capability holds significant promise for applications in collaborative robotics, autonomous systems, healthcare monitoring, among others. However, there are also potential downsides. Our method risks propagating irrelevant contextual information among entities that merely happen to be co-located but share no collective pattern, leading to "hallucinated" interaction predictions. Moreover, group-level clustering may inadvertently propagate systemic biases, particularly in scenarios requiring differential treatment of individuals within clusters (*e.g.*, unfair reward and punishment allocation in crowd behavior analysis). Hence, it is essential to rigorously consider legal regulations and integrate certain fairness constraints to avoid potential negative societal impacts.

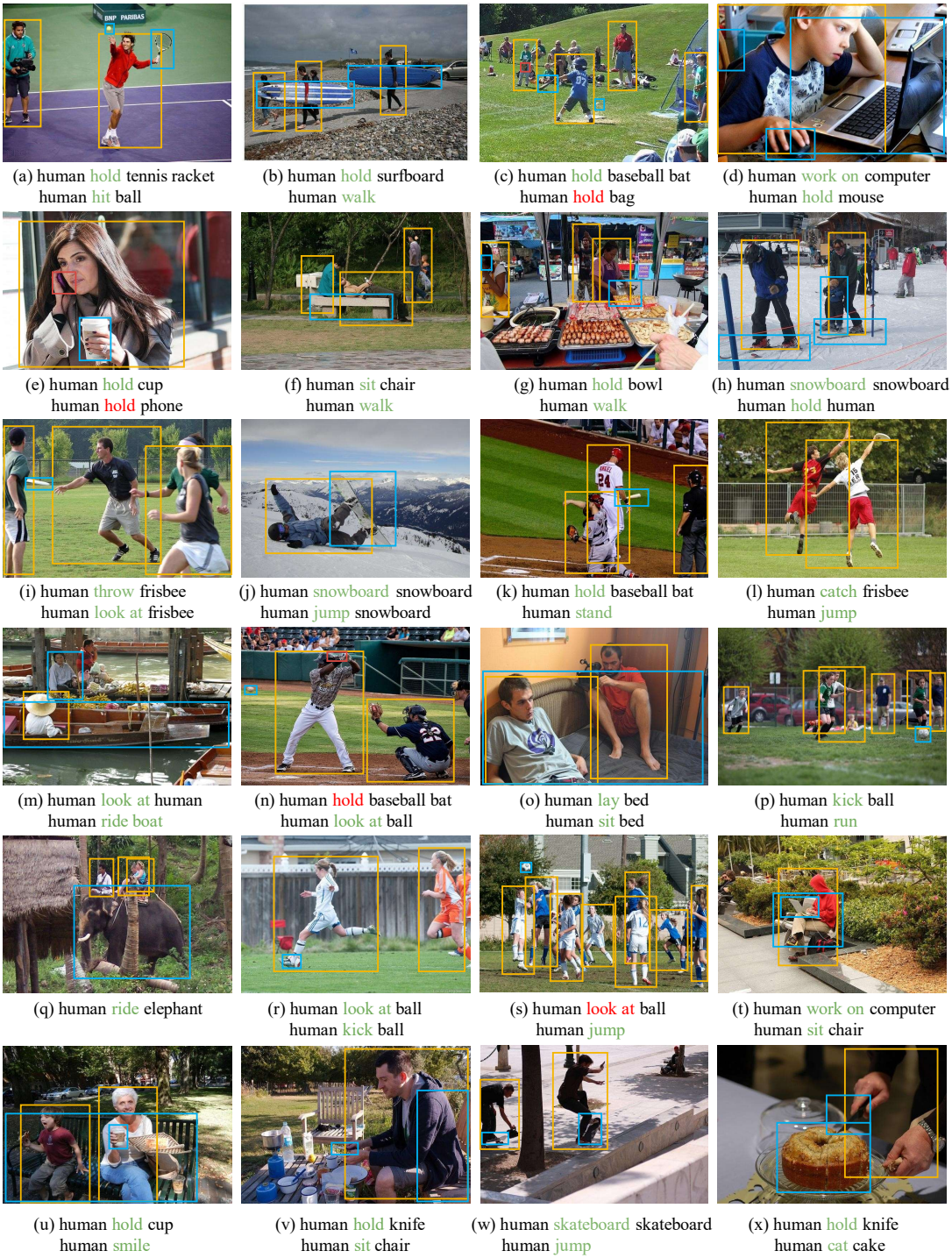

(a) human hold tennis racket
human hit ball

(b) human hold surfboard
human walk

(c) human hold baseball bat
human hold bag

(d) human work on computer
human hold mouse

(e) human hold cup
human hold phone

(f) human sit chair
human walk

(g) human hold bowl
human walk

(h) human snowboard snowboard
human hold human

(i) human throw frisbee
human look at frisbee

(j) human snowboard snowboard
human jump snowboard

(k) human hold baseball bat
human stand

(l) human catch frisbee
human jump

(m) human look at human
human ride boat

(n) human hold baseball bat
human look at ball

(o) human lay bed
human sit bed

(p) human kick ball
human run

(q) human ride elephant

(r) human look at ball
human kick ball

(s) human look at ball
human jump

(t) human work on computer
human sit chair

(u) human hold cup
human smile

(v) human hold knife
human sit chair

(w) human skateboard skateboard
human jump

(x) human hold knife
human cat cake

Figure S1: Visualization of GroupHOI results on V-COCO [18] `test`. Detected interactions are marked in Green, while missed interactions and objects are in Red.